Two Body $\bar{p}p$ Decays into
All Neutral Final States

Gunter Folger

Universität München

representing the Crystal Barrel Collaboration

Abstract

The Crystal Barrel Collaboration is analyzing $\bar{p}p$-annihilation at rest in liquid hydrogen into two neutral mesons (π°, η, ω, and η'). The status of the ongoing analysis is shown.

1 Introduction

The two main physics motivations to study $\bar{p}p$-annihilation at low energies and at rest are meson spectroscopy including the search for exotic states like glueballs and hybrid mesons, and a study of the annihilation dynamics itself. The latter is not well understood, as it involves non-perturbative QCD. In most models the $\bar{p}p$-annihilation into two or three mesons proceeds either via rearrangement of the constituent quarks (Fig 1a), or via annihilation of constituent quark antiquark pairs (Fig 1b). To decide which of the graphs dominates in $\bar{p}p$-annihilation many branching ratios for annihilation into two or three mesons need to be measured. Experimentally many of the branching ratios involving π°, η, ω, and η' are not well measured and some of the existing measurements are inconsistent, see table 1 or ref [1] for a review. The Crystal Barrel experiment has started a survey for $\bar{p}p$-annihilation into two mesons with the aim to measure many branching ratios with high accuracy.

Furthermore in both classes of models production of $s\bar{s}$ mesons (e.g. ϕ) together with non-strange mesons is suppressed. The experimental branching ratio for $\bar{p}p\rightarrow\phi\pi^\circ$ seems to violate this suppression by a factor of ten.

2 The Experiment

The Crystal Barrel detector covers nearly 4π sr and measures both charged particles and photons with good resolution. It consists of a liquid hydrogen target, two cylindrical proportional wire chambers (not installed for the data shown here), a cylindrical jet drift chamber of 30 sectors with 23 layers of sense wires each, and a barrel shaped electromagnetic calorimeter consisting of 1380 cesium iodide crystals, each 16 radiation length long. The chambers detect and measure charged particles in 92% of 4π sr. The electromagnetic calorimeter detects particles in 97% of 4π sr and measures photons with an energy resolution of $2.7\%/\sqrt[4]{E(\text{GeV})}$. The angular resolution for photons varies with the photon energy from 20 mrad to 30 mrad. The detector is surrounded by a coil and iron return yoke for a homogeneous solenoidal field of up to 1.5 Tesla. For more details see [2].

The data shown here were taken with antiprotons stopping in the liquid hydrogen target. In 1989 and 1990 we recorded $8 \cdot 10^6$ minimum bias triggers and 10^7 zero prong triggers. The zero prong trigger selects events without hits in one of the inner four layers of the jet drift chamber. So far we have analyzed only (10-20)% of the recorded zero prong data.

Table 1: Branching ratios BR for $\bar{p}p$-annihilation at rest in liquid hydrogen.

Channel	BR			Ref	Channel	BR			Ref
$\pi^\circ\pi^\circ$	2.06	±	0.14	10^{-4}	[6]	$\pi^\circ\eta'$	5.0	±	1.9	10^{-4}	[10]
	1.4	±	0.3	10^{-4}	[7]	$\eta\eta$	8.1	±	3.1	10^{-5}	[11]
	2.5	±	0.3	10^{-4}	[8]		1.6	±	0.8	10^{-3}	[12]
	4.8	±	1.0	10^{-4}	[9]	$\eta\omega$	1.0	±	0.1	10^{-2}	[11]
$\pi^\circ\eta$	4.6	±	1.3	10^{-4}	[10]		4.4	±	1.4	10^{-3}	[12]
	1.33	±	0.27	10^{-4}	[11]	$\omega\omega$	1.4	±	0.6	10^{-2}	[7]
$\pi^\circ\omega$	5.2	±	0.5	10^{-3}	[10]						

3 The Four Photon Final State

Here one can observe $\bar{p}p$-annihilation into $\pi^\circ\pi^\circ$, $\pi^\circ\eta$, $\pi^\circ\eta'$, $\eta\eta$, and $\eta\eta'$. To analyze the four photon events we select events with four photon candidates fully contained in the calorimeter and check for energy and momentum conservation by a 4-C kinematic fit. For the selected events we plot all possible combinations of $m_{\gamma\gamma}$ versus $m_{\gamma\gamma}$ of the four photons (Fig 2a). A signal for $\pi^\circ\pi^\circ$ events is evident. To enhance the other decay channels we remove $\pi^\circ\pi^\circ$ event candidates and plot for the remaining events $m_{\gamma\gamma}$ vs $m_{\gamma\gamma}$ (Fig 2b). Signals for $\pi^\circ\eta$, $\pi^\circ\eta'$, and $\eta\eta$ events are visible now.

Note that all the above decays are forbidden from atomic S-states (L=0). These decays stem from annihilation of $\bar{p}p$ in P-states (L=1). The $\pi^\circ\pi^\circ$ decay branching ratio is related to the well measured $BR_{L=1}(\bar{p}p\to\pi^+\pi^-) = (4.81 \pm 0.49) \cdot 10^{-3}$ from atomic P-states [3] by

$$B_{L=1}(\pi^+\pi^-) = 2B_{L=1}(\pi^\circ\pi^\circ) = 2f_P^{-1}B_{Liquid}(\pi^\circ\pi^\circ) \tag{1}$$

where f_P is the fraction of $\bar{p}p$-annihilation from atomic P-states in liquid hydrogen into any final state. A precise determination of the $\pi^\circ\pi^\circ$ rate in liquid hydrogen will yield f_P.

The above branching ratios also test the model of annihilation dominance (Fig 1a). There are relations for the phase space corrected branching ratios σ like [4]

$$\sigma(\eta\eta) = x^4\sigma(\pi^\circ\pi^\circ) \tag{2}$$

where x is related only to the pseudoscalar mixing angle Φ_{PS} and has a value of $x^2 = 0.72\ (0.51)$ for $\Phi_{PS} = -23^\circ\ (-10^\circ)$. The existent measurements for $\pi^\circ\pi^\circ$ and $\eta\eta$ are, given the large errors, still consistent with the prediction of equ.2.

4 The Five Photon Final State

In this final state the dominant $\bar{p}p$ decays are $\pi^\circ\omega$ and $\eta\omega$. Similar to the four photon final state we select events with five photon candidates and check energy and momentum conservation by a 4-C kinematic fit. For all 15 combinations of $(\gamma\gamma)$ $(\gamma\gamma)$ γ of the five photons we plot the mass of one $(\gamma\gamma)$ pair vs. the other pair (Fig.3). There are two clear peaks of events for $\pi^\circ\pi^\circ\gamma$ and for $\pi^\circ\eta\gamma$. Using the events in the peaks to plot the $\pi^\circ\gamma$ invariant mass distribution, prominent signals for $\pi^\circ\omega$ and $\eta\omega$ show up (Figs.4a and 4b). A fit of the above signals yields, after detection efficiency correction, the preliminary ratio

$$r = \frac{BR(\bar{p}p\to\pi^\circ\omega)}{BR(\bar{p}p\to\eta\omega)} = 0.46 \pm 0.10 \tag{3}$$

Studies of systematic effects are still in progress.

Again the model of annihilation dominance predicts relations for the phase space corrected branching ratios [4]

$$x^2\sigma(\pi^\circ\rho^\circ) = \sigma(\eta\omega) \quad \text{and} \quad x^2\sigma(\pi^\circ\omega) = \sigma(\eta\rho^\circ) \tag{4}$$

In the ratios $\sigma(\pi^\circ\rho^\circ)/\sigma(\pi^\circ\omega)$ and $\sigma(\eta\omega)/\sigma(\eta\rho^\circ)$ the phase space correction factors cancel, as ρ° and ω have the same momenta. It then follows

$$\frac{BR(\bar{p}p\to\pi^\circ\rho^\circ)}{BR(\bar{p}p\to\pi^\circ\omega)} = \frac{BR(\bar{p}p\to\eta\omega)}{BR(\bar{p}p\to\eta\rho^\circ)} \tag{5}$$

The existing measurements have too big errors to draw conclusions on the validity of the model of annihilation dominance.

The ratio $BR(\bar{p}p\to\pi^\circ\phi)/BR(\bar{p}p\to\pi^\circ\omega)$ tests the quark line rule, for a discussion see [5].

5 The Six Photon Final State

In this channel there are in addition to the $\bar{p}p\rightarrow\omega\omega$ decay many three meson final states present. To measure the $\omega\omega$ branching ratio we use the sample of candidate six photon events, select events with two π° candidates and reject events compatible with $3\pi^\circ$ or $2\pi^\circ\eta$. For the events fulfilling these criteria we plot all combinations of $m_{\pi^\circ\gamma}$ versus $m_{\pi^\circ\gamma}$ (Fig.5). Events of type $\bar{p}p\rightarrow\omega\omega$ clearly are present, but to calculate the branching ratio further studies are necessary.

Here the annihilation dominance model predicts

$$BR(\bar{p}p\rightarrow \omega\omega) = BR(\bar{p}p\rightarrow \rho^\circ\rho^\circ) \tag{6}$$

which does not seem to be the case experimentally, even given the large uncertainty on the measured BR($\bar{p}p\rightarrow\omega\omega$).

6 Summary

An analysis of $\bar{p}p$ decays at rest into two neutral mesons (π°, η, ω, and η') is currently performed using the Crystal Barrel detector at LEAR. The large solid angle coverage and the excellent energy resolution for photons enable the full reconstruction of events containing several of these mesons. This will result in measurements of many branching ratios with small errors. These branching ratios will allow to constrain models describing $\bar{p}p$-annihilation .

References

[1] C.Amsler, F.Myhrer, CERN-PPE/91-29, to be published in Annual Review of Nuclear and Particle Science 41 (1991)

[2] E.Aker et al., CERN/PSCC/P90, Experiment PS 197 (1985)

[3] M.Doser et al., Nucl. Phys. A486 (1988) 493

[4] H.Genz et al., Z. Phys. A335 (1990) 87

[5] T.Kiel, these proceedings.

[6] L.Adiels et al., Z.Phys. C42 (1989) 15

[7] G.Bassompiere et al., IV European Antiproton Symposium (1978), Vol.1, p. 139

[8] M.Chiba et al., Phys. Lett. B202 (1988) 447

[9] S.Devons et al., Phys. Rev. Lett. 27 (1971) 1614

[10] M.Chiba et al., Phys. Rev. D38 (1988) 2021

[11] L.Adiels et al., Z. Phys. C42 (1989) 49
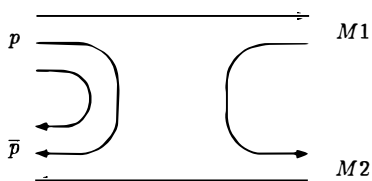
[12] M.Chiba et al., Phys. Rev. D39 (1989) 3227
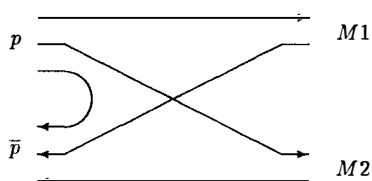
Figure 1: Annihilation (a) and rearrangement (b) diagrams of $\bar{p}p$-annihilation into two mesons.

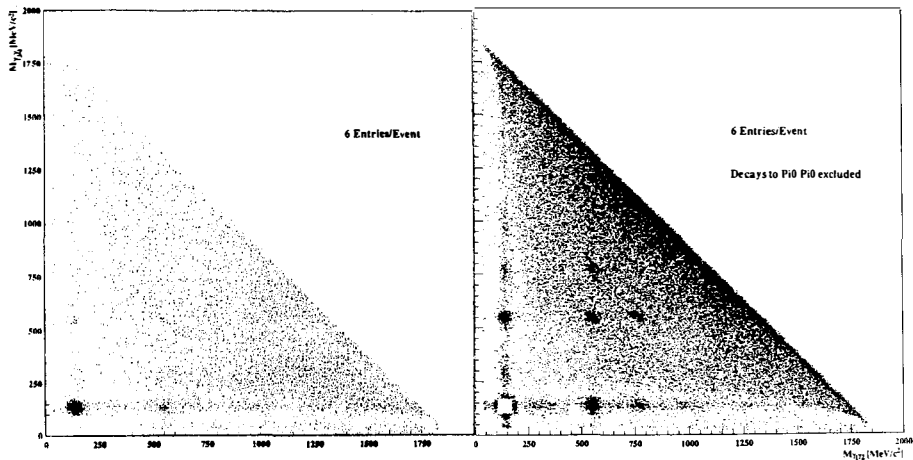Figure 2: a) $m_{\gamma\gamma}$vs. $m_{\gamma\gamma}$for all four photon events, and 2b) as above but $\pi^\circ\pi^\circ$ events removed.
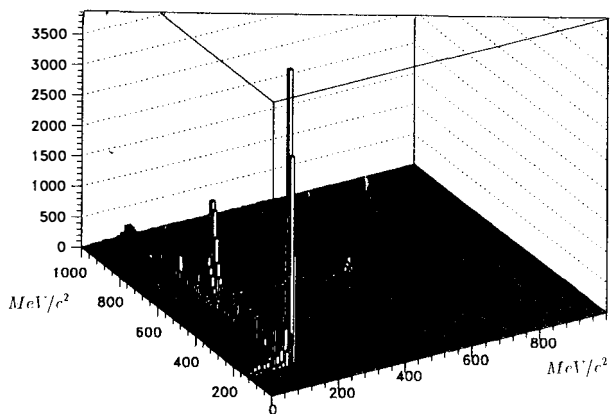

Figure 3: $m_{\gamma\gamma}$ vs. $m_{\gamma\gamma}$ for five photon events using all 15 combinations of $(\gamma\gamma)$ $(\gamma\gamma)$ γ. The entries are sorted such that the first pair always is the pair with the higher mass.
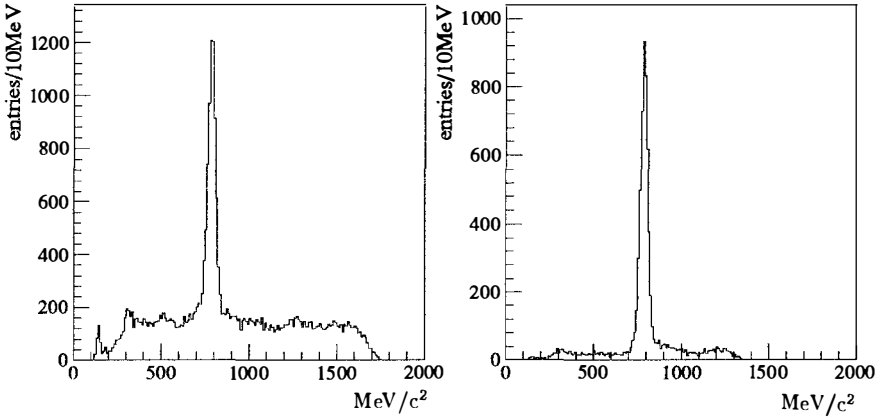
Figure 4: a) $m_{\pi^\circ\gamma}$ for $\pi^\circ\pi^\circ\gamma$ events. Two entries per event. Most of the events can be explained as $\pi^\circ\omega$.
b) $m_{\pi^\circ\gamma}$ for $\pi^\circ\eta\gamma$ events. One entry per event. Again most of the events can be explained as $\eta\omega$.
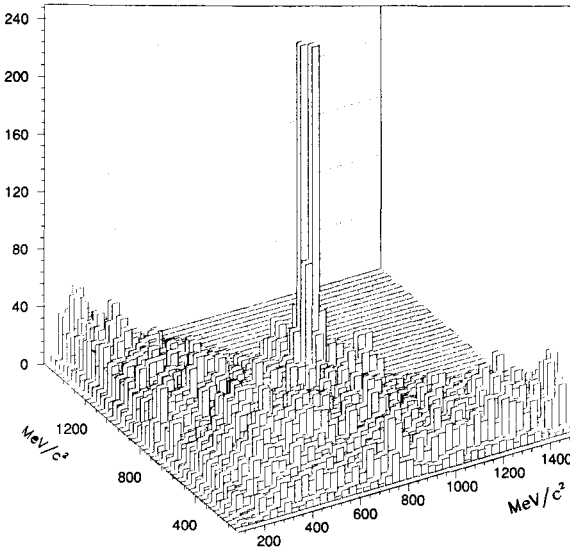

Figure 5: $m_{\pi^\circ\gamma}$ vs. $m_{\pi^\circ\gamma}$ for $\pi^\circ\pi^\circ\gamma\gamma$ events (six photon events).